Research Article

Journal of Environmental Nanotechnology

Mechanical and Microstructural Enhancement of Eco-friendly Cement Composites Using Treated Coir Fiber, Bagasse Pulp and Silicon Dioxide Nanoparticles

N. Devendran*, T. S. Lakshmi and M. K. Muniyasamy

Department of Civil Engineering, Saveetha School of Engineering, Saveetha Institute of Medical and Technical Sciences, Chennai, TN, India

Received: 29.04.2025 Accepted: 23.05.2025 Published: 30.06.2025

*nmdev24@gmail.com

ABSTRACT

The research aims to improve and detail the characteristics of cement composite boards reinforced with recycled coir fiber, bagasse pulp, and nano-SiO_2 for use in building projects in developing countries. Though it is easily accessible in many places, coir fiber (*Cocos nucifera*) has issues bonding strongly to the cement matrix. In order to modify the fiber characteristics prior to reinforcing, a mild treatment was implemented, which used varying alkali concentrations. Alkali (NaOH) treatment considerably enhanced the tensile strength of fibers, Young's modulus, thermal stability, thermogravimetric analysis and the single fiber tensile test. The laboratory-simulated Hatschek technique was employed to fabricate cement composite boards that contained varying proportions of treated and untreated coir fiber (5–15 wt %). The three-point bending tests were used to analyze the mechanical behaviour of the boards. Results demonstrated that treated fiber-reinforced composites had much higher flexural strength and ductility than untreated fiber-reinforced composites. Reinforced with treated fibers, the composites proved to be exceptionally strong, surpassing the minimum criteria of standards for fiber cement boards. The composite boards that contained 19 wt%, 1 wt %, and 5 wt % of bagasse pulp, nano-SiO_2, and treated coir fibers, respectively, achieved an optimal flexural strength of 10.66 MPa. This investigation demonstrates that the mechanical performance and behavior of cement fiber composite boards can be improved by the effective augmentation and repurposing of recycled coir fibers as reinforcement.

Keywords: Natural fiber; Nano-SiO_2; Alkali treatment; Mechanical properties; Low-cost housing; Construction industry.

1. INTRODUCTION

Natural fiber composites are gaining attention for eco-friendly construction due to their renewability and non-toxicity. Surface treatments improve fiber-matrix bonding, which in turn boosts strength and durability in mortar applications. Treated hemp composites often outperform untreated samples (Siouta *et al.* 2024). The incorporation of water hyacinth fibers enhances tensile strength and toughness, while also lowering carbon emissions. Studies on mechanical performance, such as compressive, tensile, and flexural strengths (CS, TS and FS) are vital for understanding viability. This approach supports sustainable construction with reduced environmental impact (Dutta *et al.* 2024). Wood–cement composites can significantly reduce the environmental footprint of building materials. Studies show improvements in strength when treated wood and eco-additives like nanocellulose are used. Reviews highlight a shift towards sustainability in composite research. These materials are ideal for non-structural applications with reduced cement content (Maier *et al.* 2024). Various fiber-reinforced concrete (FRC) systems using natural, recycled, and nanomaterial-based fibers to enhance mechanical performance and sustainability were explored. Studies confirm improved compressive strength, strain capacity, and durability through the incorporation of cellulose nanocrystals (CNCs), nano-alumina (NA), and PVA fibers, with optimal results at 1–2 wt % CNCs and 2 % NA + 0.3 % PVA. Hybridization with nano-silica (2.5%) further improved hydration and pore structure, as validated by SEM, TEM, and XRD analyses (Mahmoud *et al.* 2024; Gavilanes *et al.* 2024; Sridhar *et al.* 2024). Additionally, the use of alternative fibers such as bamboo, coconut, and human hair, as well as recycled glass fibers and agricultural waste ash, demonstrated promising strength enhancements, environmental benefits, and freeze-thaw resistance in optimized mixes (Yeh *et al.* 2024; Mkilima *et al.* 2024).

Hybrid epoxy composites were developed using waste marble dust (4-16 wt%) as filler and coconut fibers (CF) as reinforcement. The experiments showed that 12 wt % marble dust + 16 wt % coconut fiber provided the best mechanical properties: TS: 34.27 MPa, impact strength (IS): 16.32 kJ/m² and FS: 37.23 MPa (Bothiraj *et al.* 2022). Basalt fibers (BF) modified with nano-SiO_2 and combined with microbial agents enhanced self-healing in mortar. Secondary C-S-H formation improved

fiber bonding and mechanical properties. Improved electronegativity and surface roughness promoted bacterial adhesion and calcite deposition. Crack healing and mechanical enhancement confirm the viability of the composites for durable and intelligent construction (Zhang *et al.* 2024).

Concrete beams with nano-SiO_2 (1–3 %) and steel fibers (1 %) showed significant gains in compressive, tensile, and flexural strength. Load capacity increased by 30 %, and ACI design limits were exceeded. Nano-silicon dioxide increased brittleness but steel fibers offset this by improving ductility. This hybrid system offers promising applications for structural reinforcement (Hama *et al.* 2025). Mortars with nano-SiO_2 and macro-steel/micro-polypropylene fibers resisted sulfuric acid degradation effectively. Nano-silica (NS) improved strength and compactness, while hybrid fibers bridged cracks to delay propagation. The NS particle size and fiber synergy were key to performance. These results support mortar design for harsh chemical exposure environments (Akbulut and Guler, 2024). Basalt fibers treated with ethyl positive silicate and HCl, and coated with nano-SiO_2, enhanced crack and sulfate resistance in concrete. Modified basalt fiber (M-Si-BFRC) reduced stress relaxation by 56.21 % and improved pore structure and density. Chemical bonding and surface roughness upgrades aided hydration and resistance. The method offers a novel solution for durable fiber-reinforced composites (Zhu *et al.* 2025). Recycled aggregate concrete was reinforced using hybrid systems of nano-SiO_2, BF and polypropylene fiber (PPF). This hybrid achieved top shear strength (6.99 MPa) and fracture energy (34.6 J). The 3D structure of the systems filled defects and improved hydration. Optimal contents were 3.5 % NS, 0.5% BF, and 0.1 % PPF, validated by response surface methodology (Sun *et al.* 2024).

Alkali-resistant glass fiber and quarry dust were incorporated into engineered cementitious composites (ECC) to reduce cost and environmental impact. It was observed that up to 75 % replacement of silica sand retained compressive and flexural strength. Optimal fiber volume (2%) yielded superior mechanical performance. Quarry dust is shown as a sustainable, cost-effective substitute for ECC components (Ramya and Vijayaprabha, 2024). Amsalu *et al.* (2024) reviewed and compared alkaline and pozzolanic treatments for enhancing sisal fiber in cement composites. Pozzolanic treatment outperformed alkali in boosting strength and reducing water absorption. Treated fibers improved thermal resistance and fiber-matrix bonding. Alkaline methods showed environmental concerns, reinforcing the benefits of pozzolanic alternatives. Abera *et al.* (2024) studied FRC as a sustainable and durable building solution using steel, synthetic, and natural fibers. Emphasis was placed on recycled materials and natural options like coir and bamboo to reduce environmental impact. Challenges included fiber dispersion and alkali resistance of natural fibers. Thus, emerging smart FRC applications promise intelligent and self-monitoring structures (Abera *et al.* 2024). Natural fiber composites like flax, and coir are gaining attention for replacing glass and carbon fibers in construction and automotive sectors. They offer biodegradability, low weight, and cost-effectiveness. Treatments improve their properties for wider use. This mini-review highlighted their environmental benefits and growing industrial relevance (Palanisamy *et al.* 2024). Mahboob *et al.* (2024) experimentally evaluated concrete mixes incorporating recycled aggregates and fibers (steel, plastic, kenaf). Fiber-reinforced concrete variants improved flexural strength, toughness, and freeze-thaw resistance. Recycled steel fiber mix showed the highest compressive and durability metrics. These findings show potential of FRC as sustainable, high-performance construction materials. Yang *et al.* (2024) examined low-carbon, high-performance cement-based composites as a solution to the limitations of traditional and ultra-high-performance concrete. Materials like LC3, inert fillers, alkali-activated binders, and recycled fibers are explored for improved sustainability. Nanomaterials and chemical additives enhance properties and expand applications. Life-cycle assessments confirm the superior environmental and structural benefits of these low-carbon composites.

Ghosh *et al.* (2024) evaluated the effect of coconut fiber (0–1 %) and recycled concrete aggregate (RCA) (25–100 %) on pervious concrete. Results showed improved CS and FS at 1 % fiber without compromising permeability. Aggregate size influenced strength, especially with RCA. The approach supports durable, eco-friendly pavements for stormwater management. This study produced paving blocks with mixed Construction and Demolition Waste (CDW) and 0.1 % coconut fiber across varying water-cement ratios. Tests showed improved compressive strength and water absorption for mixes with CDW and CF. Results support the application of these blocks for light traffic pavements. Use of waste materials enhances sustainability (Brasil *et al.* 2024). Concrete with 50–100 % recycled aggregates and 2 % coconut fiber was tested with/without superplasticizer (SP). Coconut fiber improved shear strength by up to 60% and enhanced mechanical performance when combined with SP. Durability concerns like permeability were mitigated using SP. Scanning electron microscopy showed that CF bonded well, with no degradation over 1 year (Ali *et al.* 2022). Bagasse pulp was treated with 1–4 % styrene acrylate emulsions; 3 % hard PSA showed peak performance. Tensile strength improved by 13 % (to 38 MPa) and breaking length by 64 % (to 67 m) compared to untreated paper. Emulsion particles were 182 nm in size with a T_g of 26.8 °C. UV exposure reduced strength due to aromatic group degradation (Morsi *et al.* 2024). Filaments with up to 40 w t% bagasse fibers and 6% bio-based compatibilizer achieved CO_2 storage of 2.12 kg CO_2-eq/kg. Energy absorption increased with fiber

content. Mechanical properties were significantly improved, while water absorption increased up to 10 %. The 3D-printed shapes confirmed structural viability, and life cycle assessment validated reduced emissions and increased CO_2 sequestration (Ehman *et al.* 2020).

2. MATERIALS AND METHODS

2.1 Materials

Table 1. Specifications of the materials (Bheel *et al.* 2024; Zhang *et al.* 2020)

Specification	Range
Lignin	45.7
Cellulose	43.5
Pectin related compound	3.3
Hemicellulose	0.2
Water soluble	5.2
Ash	2.2
Portland Cement	
SiO_2	20.77
Al_2O_3	5.10
Fe_2O_3	3.16
CaO	60.21
Na_2O	0.17
SO_3	2.85
Loss on Ignition	2.44
Specific gravity	3.12
Nano SiO_2	
Grain diameter	15 nm
Specific surface area	250 m/g

Therefore, the objective of the current study is to utilize recycled fibers to produce ecofriendly composite boards for potential use in building applications in developing countries. Hence, the study examines how different alkali concentrations impact the properties of recycled coir fiber as well as their reinforcement efficiencies in cement composite boards produced using a unique method designed to mimic the industrial Hatschek process for fiber cement board (FCB) production. This study examined and reported the effects of treatment with 1, 2, and 3 M alkali concentrations for 2 hours at ambient laboratory temperature. Additionally, the reinforcing capability (bagasse pulp with nano-SiO_2) of treated and untreated fibers at varied percentages of 5, 10, and 15 wt % was investigated and reported.

Coir fibers (Fig. 1) were collected through the separation of the coconut husk, followed by the extraction of fibers using mechanical decorticating machine. After extraction, the fibers were thoroughly cleaned to remove residual pith and other impurities, and subsequently dried under controlled conditions to ensure optimal quality for further processing. Nano-SiO_2 particles were procured from GoGreen Enterprises, Chennai, Tamil Nadu, India. Bagasse pulp was derived from sugarcane byproducts.

Ordinary Portland cement CEM I 52.5 N, classified as high-strength (HS52) cement according to BS EN 197-1 was used. Deionized water (DI-water), pH meter, rectangular steel mold, vacuum pump, conical flask, and additional materials for simulating the Hatschek process were acquired from the Global scientific company, Erode, Tamil Nadu, India. Table 1 shows the specifications of materials used in this study.

2.2 Preparation of Fiber

The extraction of coir fibers involves the mechanical or manual processing of coconut husks to separate the fibers from the pith and outer shell. Initially, mature coconut husks were collected and subjected to a retting process, wherein they were soaked in water for 2 hours to soften the husk material. Following retting, the fibers were extracted manually by beating with wooden mallets using decorticating machines. The extracted fibers were subsequently washed to remove adhering pith and impurities, and then dried under natural sunlight.

2.3 NaOH Treatment

In alkali treatment, the type of alkali, concentration, and curing time are critical (Mahmood *et al.* 2024). To ensure the entire length of the fiber was submerged in the alkali solution and to attain uniform fiber treatment, the alkali solution-to-fiber ratio was sustained at 25:1 vol/wt. The extracted fibers were subjected to treatment for 2 hours at ambient temperature with varying amounts of alkali solutions at 1, 2, and 3 M concentrations. The residual alkali solution was eliminated from the treated fibers by thoroughly rinsing them with flowing tap water for 15 to 20 minutes or until a pH of less than 8.0 was attained. Subsequently, the fibers were cleansed again with deionized water. After rinsing, the fibers were allowed to air dry in the laboratory for a minimum of 48 hours before being securely packaged in zip bags and stored appropriately. Similarly, optimal strength improvements were observed with 15 g/L NaOH and KOH at 14–28 days.

2.4 Tensile Properties of Coir Fibers

Utilizing a Leica 0.5x microscope, the DEBEN microtester MT200 single leadscrew tensile tester was employed to calculate the tensile strength and Young's modulus (YM) of both treated and untreated recycled coir fibers. In compliance with the requirements of ASTM D3822-07, a 5 N load cell was used with a 10.2-mm gauge length flexible cardboard mounting card and a motor speed of 0.1 mm/min. Each case included five specimens of the individual combination, and the mean results were recorded.



Fig. 1: Extraction of coir fibers

2.5 Preparation of Bagasse Pulp

The production of bagasse pulp for use in coir fiber reinforced cement composites begins with the collection of sugarcane bagasse, the fibrous by-product left after juice extraction. The bagasse was oven-dried at approximately 60–80 ℃ to reduce its moisture content below 10%. Once dried, it was chopped into small pieces of about 1–2 cm in length to facilitate pulping. The chopped bagasse was then soaked in potable water for 48 hours to soften its lignocellulosic structure. After submerging, the softened material was mechanically pulped for 2 hours. Subsequently, it underwent low-speed grinding in a table-top mixer for a further 8–10 minutes. This pulp was sieved to remove larger undigested particles, ensuring uniform fiber size. The excess water was then manually squeezed out from the pulp using a muslin cloth or filtration, and the resulting semi-wet pulp was stored in sealed zip-lock bags at 4 ℃.

2.6 Fabrication of Coir Fiber Cement Composite Boards

Both treated and raw coir fibers were used to create fiber-reinforced cement composite boards of varying compositions (5, 10, and 15 wt %) using the simulated Hatschek process. The individual materials (bagasse pulp, nano SiO_2, recycled coir fiber, and cement) were weighed in accordance with the mix design illustrated in Table 2 using the Scout Pro digital weighing balance. Then, the fibers (treated and untreated) were manually chopped into short fibers of 20 mm in length (Zhang *et al.* 2020). Recycled coir fibers were reused in mortar, maintaining good performance at 12.5 % fiber content. The dense mesh (2.5×1.25 cm) showed superior stiffness and energy absorption, with moderate insulation benefits (Majumder *et al.* 2024).

Table 2. Experimental combination of coir fiber, bagasse pulp, nano SiO_2 cement board composite

S. No.	Sample Code	Cement (wt %)	Bagasse Pulps (wt %)	Nano SiO_2 (wt %)	Untreated Coir Fibers (wt %)	Treated Coir Fibers (wt %)
1	S0	200	0	0	0	0
2	S1	190	9.5	0.5	0	0
3	S2	180	19	1	0	0
4	S3	170	28.5	1.5	0	0
5	S4	160	38	2	0	0
6	S5	175	19	1	5	0
7	S6	170	19	1	10	0
8	S7	165	19	1	15	0
9	S8	175	19	1	0	5
10	S9	170	19	1	0	10
11	S10	165	19	1	0	15

Fiber cement composite boards were made by mixing a specific weight of bagasse pulp with water for three minutes using a portable handheld mixer running at 600 to 1,900 rpm. This is to ensure that the bagasse pulps are uniformly disseminated throughout the water. Following this, calculated amount of bagasse pulp blend, nano SiO_2, recycled coir fiber and the cement matrix were thoroughly blended for an additional 3–5 minutes

to ensure homogeneity. The durability and fracture behavior of high-ductility concrete were studied with various nano silica (NS) contents (Li *et al.* 2025). The slurry was poured into the preassembled rectangular steel mold of dimensions 180 × 80 mm in a successive layer after mixing.

The excess water in the combined sediment was subsequently removed from the mold by utilizing the vacuum device that was attached to the mold. Surplus water was sucked into a conical vessel that was affixed to one end of the mold. The specimen was compressed and the residual water retained in the thickened sediment was eliminated by applying a consistent weight of 12 kg to the mold. Approximately 15–20 minutes were allowed for the specimen to air dry before it was transferred to a high-humidity chamber for curing and cement hydration. A flat rectangular surface was used to deform the specimen manually. The vacuum pump was turned off after approximately 2–3 minutes of removing the excess water. The FCB specimens were allowed to endure the cement hydration process and curing in the high humidity chamber at 95 % relative humidity and 25 ℃ for 7, 14, and 28 days. Flexural strength and ductility experiments were conducted on the cured FCB specimens after 7, 14, and 28 days of hydration in accordance with the BS EN 12467 (BSI 2012) standards. For each composite design, a total of 15 specimens were manufactured. The evaluation of five of these specimens was conducted after seven days, five more after fourteen days, and the remaining five after 28 days of curing. Specimens vary in thickness from 8 to 10 mm.

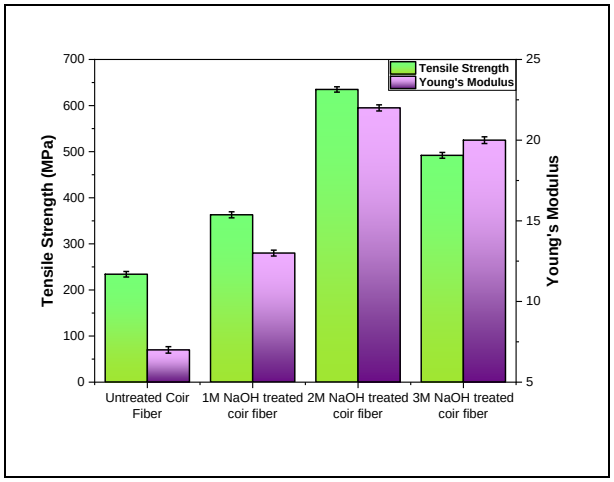


Fig. 2: Evaluation of TS and YM of raw and NaOH-treated coir fibers

2.7 Analysis of Composites Comprised of Treated and Raw Coir Fiber

2.7.1 Thermogravimetric Analysis

The Q500 TA thermogravimetric analysis (TGA) instrument was employed to record the thermal properties of the treated and untreated coir fibers in a nitrogen atmosphere using the ramp method. A heating rate of 10 ℃/min was maintained within the temperature range 30 ℃ – 600 ℃ (Abou and Kamel, 2023).

Table 3. Tensile properties of raw and NaOH-treated coir fiber

Sample	TS (MPa)	YM (GPa)	Elongational Break (%)
Raw coir fiber	234	7 ± 0.2	3.14 ± 0.12
Coir fiber treated with 1 M NaOH	363	13 ± 0.18	1.95 ± 0.115
Coir fiber treated with 2 M NaOH	635	22 ± 0.19	1.92 ± 0.09
Coir fiber treated with 3 M NaOH	492	20 ± 0.21	3.14 ± 0.097

2.7.2 Analysis of Flexural Properties

A three-point bending/flexural test was conducted on the cured specimens using the Instron 4467 electromechanical testing equipment in accordance with the BSI 2012 standard. The span of the supports was sustained at 130 mm throughout the test. Modulus of rupture (MOR) is the conventional term used to describe the FS of coir fiber cement board. It was evaluated by the expression in Eq. (1) (Lamichhane *et al.* 2024).

$$MOR = \frac{3FL_S}{2be^2} \quad \ldots (1)$$

whereas

L_s = Denotes the span (mm) between the axes of the two supports
F = Indicates the breaking load (N)
e = Denotes the sample thickness (mm)
b = Represents the sample width (mm)

3. RESULTS AND DISCUSSION

3.1 Results on Tensile Properties of the Raw and NaOH-treated Coir Fiber

Fig. 2 and 3 shows the TS and YM of raw and NaOH-treated coir fibers with varying concentrations of NaOH. Table 3 provides the tensile properties of the NaOH-treated and raw coir fiber.

It was noted that the TS and YM of the NaOH-treated coir fibers rised as the alkali concentrations increased up to 2 M, and then gradually decreased at a concentration of 3 M. The tensile properties of the alkali-treated coir fibers were enhanced as a consequence of the removal of the cementing material lignin from the fiber cell wall (Zhang *et al.* 2020). As a result of this removal, the internal strain was released, rendering the microfibrils of the fibers more susceptible to self-rearrangement in a more compact manner. Consequently, the tensile characteristics were enhanced as a consequence of the fibers being more closely packed. Furthermore, the TS and YM of the 1 M NaOH-treated fiber were, respectively, enhanced by 35.54 % and 46.15 % in comparison to the raw coir fiber. The YM and TS of the coir fiber treated with 2 M NaOH were both enhanced by 62 % and 69 %, respectively. However, the high concentration of NaOH solution, which initiates fiber degradation, is the cause of the progressive decrease in the TS and YM of the 3 M NaOH-treated coir fiber.

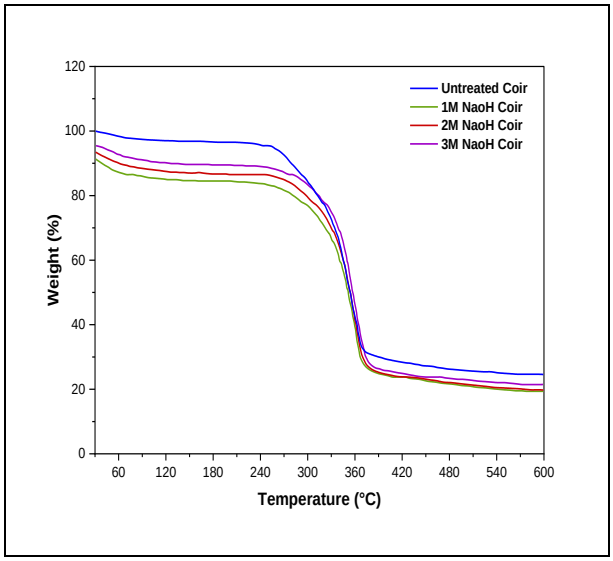


Fig. 3: TGA results for raw and NaOH-treated coir fiber

Table 4. TGA analysis results

Sample	No. of Transitions	T_i	T_f	Weight Loss at Successive Ttransition (%)	Residual Weight (%) at 600 °C
C-UT (coir untreated)	1	30	235	3.9	16.5
	2	235	366	65.7	
	3	371	580	23.2	
CT-1 (coir 1 M NaOH)	1	30	235	3.3	17.4
	2	255	376	65.6	
	3	376	580	21.2	
CT-2 (coir 2 M NaOH)	1	30	235	2.7	18.1
	2	255	376	63.9	
	3	376	580	22.0	
CT-3 (coir 3 M NaOH)	1	30	235	6.3	19.5
	2	255	376	65.6	
	3	376	580	24.6	

3.2 Results on TGA for the Raw and NaOH-treated Coir Fibers

The TGA curve of raw and NaOH-treated coir fiber, as depicted in Fig. 3, exhibited a three-stage degradation profile in accordance with the temperature ranges illustrated in Table 4. The raw coir (C-UT) sample experienced a 3.9 % weight loss during the initial stage of degradation, which is attributed to the fiber's depletion of moisture. Nevertheless, the alkali-treated fiber samples CT-1, CT-2, and CT-3 exhibited a corresponding percentage weight loss of 3.3 %, 2.7 %,

and 6.3 %. As the concentration of the alkali treatment increased, the percentage weight loss of the NaOH-treated fiber samples decreased, representing that the quantity of moisture absorbed consistently decreased. This implies that the alkali-treated fiber samples absorbed less moisture than the untreated coir fiber. This may be the result of the elimination of alkali-sensitive constituents that are also active locations for moisture absorption. This removal reduces the quantity of absorbed water as a result of a high concentration of alkali solution.

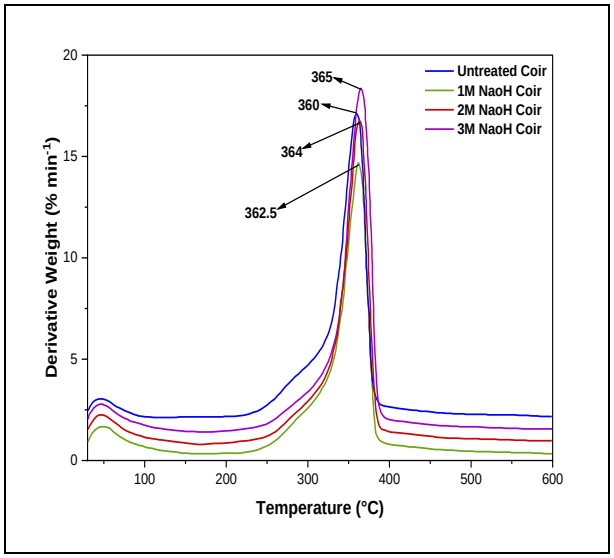


Fig. 4: TGA combustion temperature for raw and NaOH-treated coir fibers

The second stage of degradation revealed the component's decomposition in both the NaOH-treated and raw fiber samples. Table 4 illustrates that the C-UT fiber sample demonstrated the highest percentage of weight loss among all alkali-treated fiber samples, while CT-2 exhibited the lowest percentage of weight loss. The lower weight loss percentages are due to the increased alkali concentration, which leached out a significant quantity of non-cellulosic components from the treated fiber samples. In addition, it was noted that the initial and final temperatures for the second stage of degradation increased as the untreated fiber was compared to the NaOH-treated fiber samples. The NaOH-treated fiber samples at 1 M NaOH, 2 M NaOH, 3 M NaOH were able to withstand a higher temperature than the untreated fiber sample, as evidenced by this. Table 4 illustrates that the temperature of the hydration process (approximately 95 °C) is lower than the thermal degradation temperature of the treated fibers. In cement composite boards, the treated fibers remained intact even after the cement hydrates. The large loss of hemicellulose caused the fibers to lose their cementing capability, separating them from one another and resulting in a much smaller diameter. The degradation of α-cellulose is represented by the third stage of the degradation profile. The percentage residual weight at 600 °C increased consistently from the untreated fiber sample to the alkali-treated fiber samples.

The alkali-treated sample S8 exhibited the highest residual weight percentage of 19.5, as observed. Lignin and hemicellulose possess lower thermal degradation temperatures and combust more thoroughly, resulting in less char, which suggests their removal during alkali treatment. The NaOH treatment increased the char content by diminishing the fiber's hemicellulose content and creating a lignin-cellulose complex. In relation to the raw fibers, the alkali-treated fibers exhibited greater stability. Fig. 4 illustrates the temperatures at which the cellulose constituents of both alkali-treated and raw coir fibers undergo decomposition. During the second phase of the deterioration profile, as illustrated in Fig. 3 and Table 4, the degradation temperature of untreated coir fiber commences at 324 °C and concludes at 360 °C. Nevertheless, the degradation temperatures of the alkali-treated coir fiber samples at 1 M NaOH treated, 2 M NaOH treated and 3 M NaOH treated have increased from 331.5 °C to 362.5 °C, 336 °C to 364°C, and 338°C to 365°C, respectively, for the start and end of cellulosic component degradation. The alkali treatment has increased the heat resistivity of the fiber by reacting with the highly reactive inorganic material, such as sodium, present in the alkali solution. This suggests that the fiber is more heat resistant.

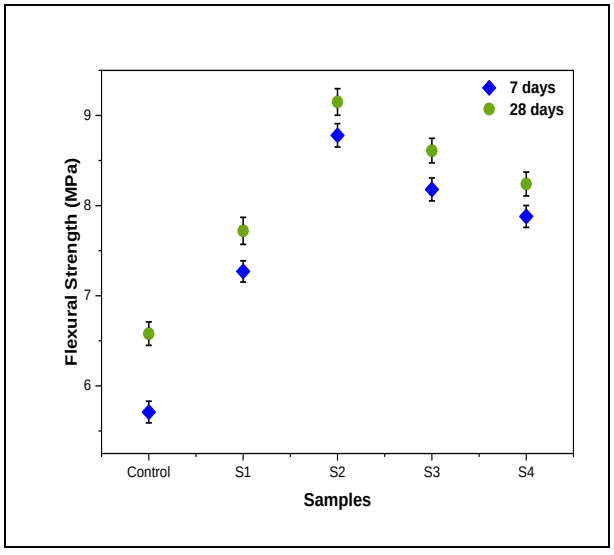


Fig. 5: Evaluation of mean FS of FCB reinforced with 0%–40% of bagasse pulp and nano-Sio_2 reinforcement (7 and 28 days)

3.3 Flexural Characteristics of Bagasse Pulp-reinforced Fiber Cement Board with Nano-SiO_2 Filler

The flexural strength or bending strength of a fiber cement composite board is a critical property, as it is a determinant of the other properties of the board. Fig. 5 illustrates the average flexural strength of the control

sample (which contains only cement matrix) and bagasse pulp-reinforced cement boards with 9.5 %, 19 %, 28.5 %, and 38 % of bagasse pulps and 0.5, 1, 1.5, and 2 wt % of nano SiO_2 by weight of cement matrix, respectively, after being hardened after first week and third week.

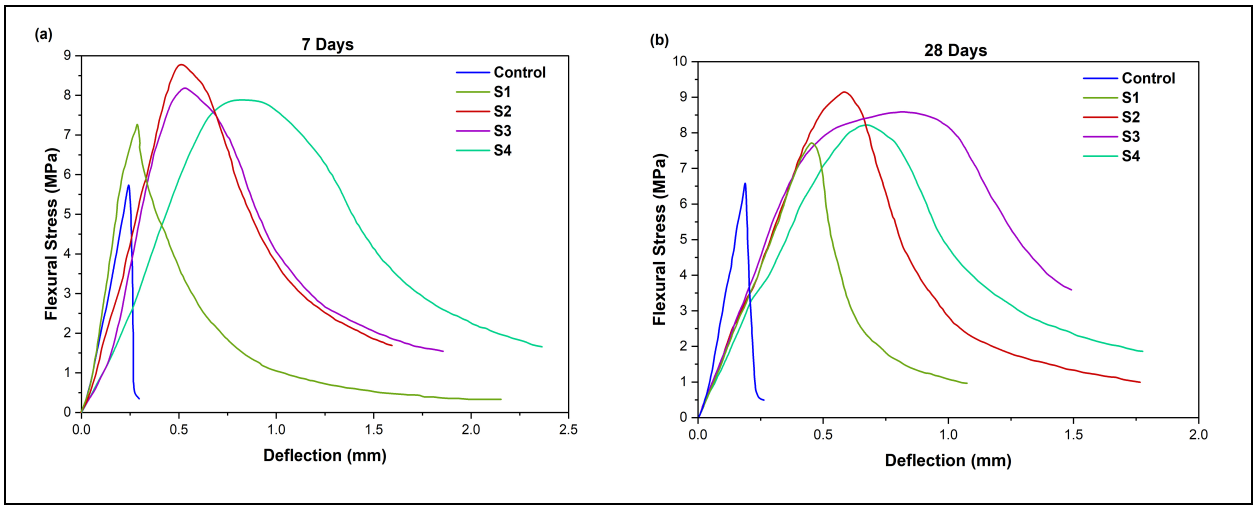


Fig. 6: Evaluation of mean flexural behavior of FCB reinforced with 0 % – 40 % of bagasse pulp and nano-SiO_2 reinforcement

All boards, including the control sample, experienced a progressive increase in FS as the number of hydration days increased from 7 to 28, as anticipated. The constant formation of cement hydration products results in an increase in the strength of a cement mortar as the number of hydration days increases. Results show that up to a 20 % reinforcement addition, the FCB's FS increased steadily and consistently with increasing reinforcement content. However, a gradual and steady decrease in flexural strength was observed at fiber additions exceeding 20 %. The uniform fiber distribution and adequate bonding at the fiber-matrix interface were responsible for the initial improvement in the flexural strength of FCB samples reinforced with 9.5% and 19 % bagasse pulp with nano-SiO_2 (0.5 % and 1 %), respectively (also known as S1 and S2). Conversely, the gradual reduction in flexural strength observed in the FCB with a fiber addition of over 20 % was a consequence of the inadequate interaction at the fiber–matrix interface, which was caused by the higher percentage of fiber reinforcement. This resulted in fiber agglomeration or the balling effect.

The balling effect is a result of the composite board's higher percentage of bagasse pulps in comparison to the number of cementitious matrix particles. This resulted in the formation of a fiber region within the composite board, which in turn created a vulnerable point within the board. Consequently, the FS of these composite samples gradually decreased. In addition, the FS value of the composite sample S1, which contained 9.5 wt % bagasse fiber and 0.5 wt % nano-SiO_2 reinforcement, was 7.27 MPa at 7 days and 7.72 MPa at 28 days. At 7 days, the strength increased by 21.46 % and 14.77% at 28 days, it increased by 28.09 % compared to the S2 sample, which had a value of 5.71 MPa. Similarly, the composite sample S2, which contained 19 % bagasse pulp and nano-SiO_2 reinforcement, exhibited a 34.97 % and 28.09 % increase in FS compared to the S2 sample at first and third week, respectively. The range of FS was in between 8.79 and 9.06 MPa. This showed that the FCB can attain the utmost FS feasible by incorporating bagasse fiber and nano-SiO_2 into the cementitious matrix to a maximum of 20 % by weight. As a result, the composite sample S2 meets the Class 2 minimum requirement (8.79 MPa) of the EN 12467 norms in terms of the MOR required for fiber cement flat sheets. Fig. 6 illustrates the flexural behavior of composite samples reinforced with 9.5 % – 38 % of bagasse pulp with 0.5 %-2% nano-SiO_2 after hydration for 7 and 28 days. The control sample's abrupt failure is attributable to the characteristic brittleness of the cement matrix, as evidenced by the brittle-fracture mechanism. Nevertheless, the composite samples that contained bagasse material and nano-SiO_2 reinforcement exhibited a distinct fracture mechanism. This demonstrates that the flexural behavior and fracture mechanism of the composite samples are influenced by the presence of the bagasse pulp and nano-SiO_2.

The deflection response of the composite sheets was found to be substantially different from that of the control sample when the fiber contents were increased from 9.5 to 38 wt %. This is because the reinforcing fibers and cementitious matrix interact at the fiber-matrix contact, allowing the load to be smoothly transferred from the cement to the fibers. Therefore, the composite samples showed a gradual transition to failure mechanism, rather than an abrupt failure. Therefore, the S2 sample, which comprises 19 wt. % bagasse pulp with 1 wt % nano-SiO_2 reinforcement by weight of the cement matrix, demonstrates the optimal flexural stress with a

deflection response of approximately 0.6 mm. Conversely, the S4 sample, which comprises 38 wt.% bagasse pulp and 2 wt % nano-SiO_2 reinforcement, exhibits the most significant deflection response, with an approximate value of 0.8 mm. Furthermore, a more detailed examination of Fig. 6 (a and b) demonstrates that the deflection response of the individual specimens was positively impacted by the extension of the hydration period of the various composites from 7 to 28 days. This is evidenced by the minor variations in the area under the stress-deflection curves of each specimen.

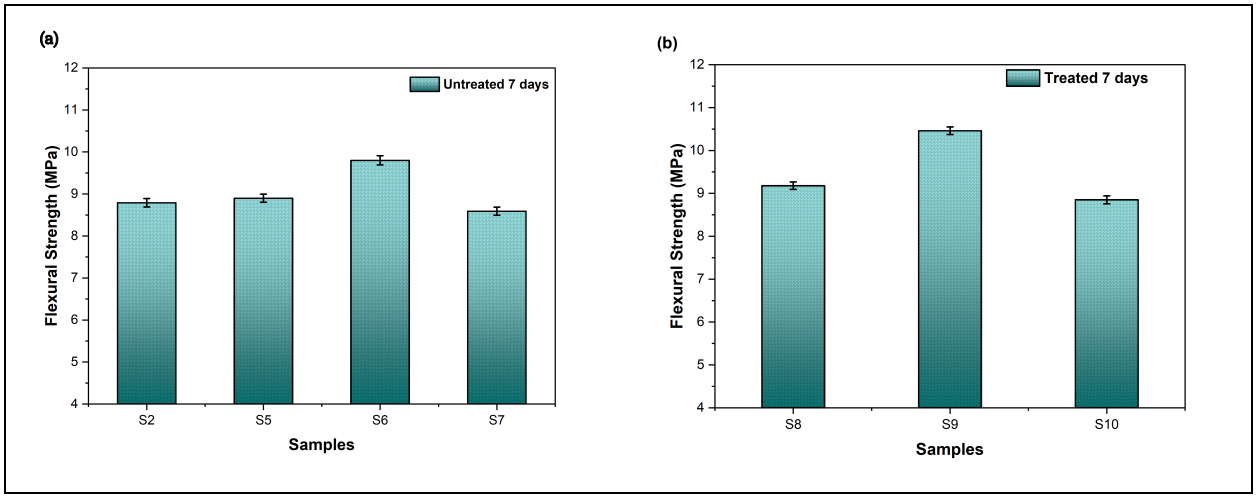


Fig. 7: Mean FS of FCB reinforced with 19 wt % of bagasse fibers +1 wt % of Nano-SiO_2, and 5 %, 10 %, and 15 % of coir fibers (7 days)

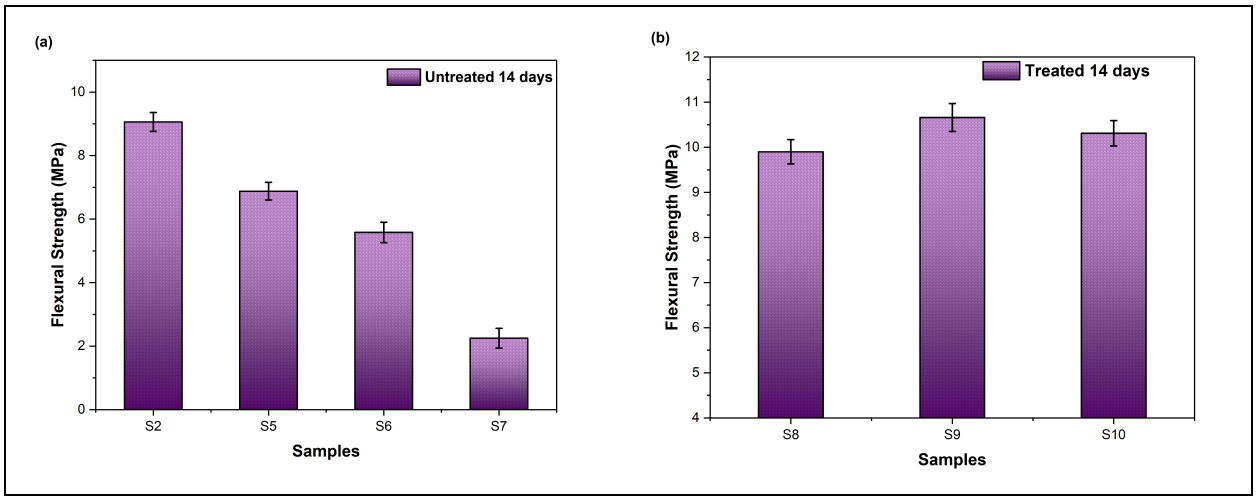


Fig. 8: Mean FS of FCB reinforced with 19 wt % of bagasse fibers +1 wt % of Nano-SiO_2, and 5 %, 10 %, and 15 % of coir fibers (14 days)

3.4 Flexural Properties of Fiber Cement Board Reinforced with Bagasse fibers + Nano-SiO_2 and Coir Fibers

Fig. 7 and 8 illustrate the FS of FCB reinforced with bagasse fibers with Nano-SiO_2, raw and NaOH-treated coir fibers. The FS of the composite sheets was considerably improved by the addition of NaOH-treated coir fiber to the cement board after 7 and 14 days of hydration. The effective interfacial bonding at the fiber-matrix interface, which was achieved due to the modified-surface morphology of the fiber as a result of the alkali pretreatment, can be attributed to the enhanced FS of the alkali-treated coir fiber-reinforced composite board. Conversely, the composite sheet reinforced with untreated coir fiber exhibited a substantial decrease in FS, particularly after 14 days of hydration. The untreated coir fiber's smooth surface, which was unable to form a strong bond with the cement matrix, is the cause of the fiber-debonding that led to a decrease in the FS of the untreated coir fiber reinforcement composite board. The maximum NaOH environment of the cement is the cause of this severe deterioration, which also contributed to the decreased FS of the composite sheet. The elevated alkalinity of the cementitious matrix causes partial dissolution of the fiber's chemical components, leading

to the production of an adverse precipitate of inorganic particles on their surface. This precipitate causes damage to the fibers and reduces their ability to reinforce. The potential for severe fiber damage was further corroborated by a visual examination of the composite sheets reinforced with the untreated coir fiber, which was indicated by the substantial weight loss observed in the composite samples after 14 days of hydration. Moreover, the FS of the composite board reinforced with the alkali-treated coir fiber increased significantly from 8.90 MPa for S2 (reference sample) to a maximum of 10.66 MPa for S6 after 14 days of hydration, as illustrated in Fig. 9. The incorporation of alkali-treated coir fiber resulted in a 20 % increase in the composite board's FS, as indicated by this. The optimal FS of S6 met the minimum requirements of the fiber-cement sheet in stage 2 in accordance with the BS EN 12467-2012 standards for fiber cement flat sheets. Fig. 9 and 10 show the flexural behavior of FCB strengthened with bagasse pulp with nano-SiO_2 and untreated and alkali-treated coir fibers after 7 and 14 days of hydration, respectively.

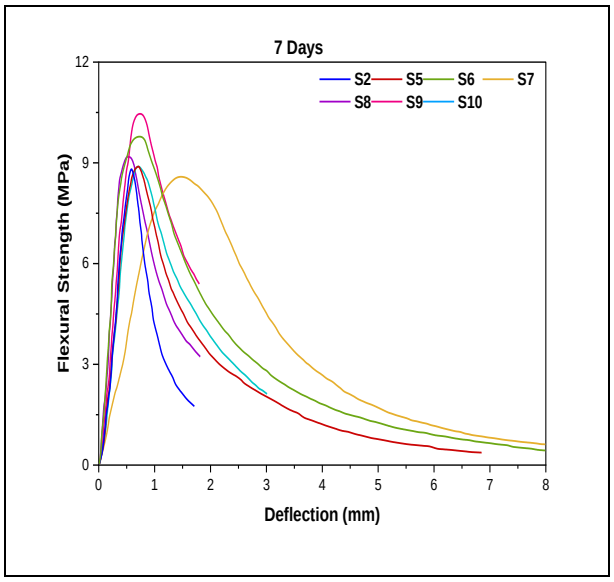


Fig. 9: Flexural behavior of FCB reinforced with 19 wt.% bagasse pulp + 1 wt % nano-SiO_2 and 5 %, 10 %, and 15 % of raw and NaOH-treated coir fibers (7 days)

Sample S2 was employed as the reference sample in these figures. This sample is composed of 19% bagasse cellulose and 1wt% nano-SiO_2 fibers by weight of the specimen. It was observed that the flexural strength of composite samples reinforced with alkali-treated coir fiber was significantly greater than that of specimens reinforced with untreated coir fiber. In addition, the FS of FCB strengthened with alkali-treated coir fiber increased progressively as the hydration period increased from 7 to 14 days. In contrast, the composite boards demonstrate a higher flexural strength than the specimens reinforced with untreated coir fiber at 7 days of hydration than at 14 days of hydration. The FS of the alkali-treated coir fiber-reinforced composite boards was improved up to 5 % fiber addition, in contrast to the untreated coir fiber-reinforced composite samples, which experienced a continuous decline in flexural strength as the fiber contents increased. Unlike the 7-day samples, the presence of lignin in the untreated coir fibers contributed to the reduction in flexural strength observed in the 14-day samples of the composite reinforced with untreated coir fiber.

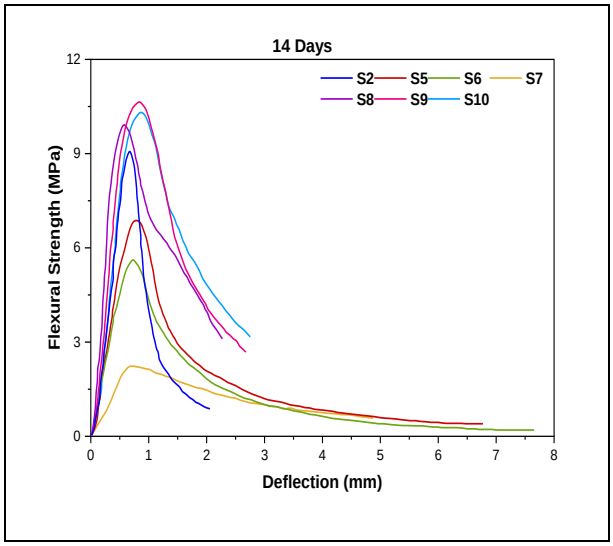


Fig. 10: Flexural behavior of FCB reinforced with 19 wt.% bagasse pulp + 1 wt % nano-SiO_2 and 5 %, 10 %, and 15 % of coir fibers (14 days)

The composite reinforced with NaOH-treated coir fibers showed a gradual increase in deflection as the fiber content improved, as demonstrated in Fig. 9 and 10. The deflection response of the composite samples S5 and S6 peaked at 1.5 and 2.3 mm, respectively, in contrast to the counterpart reinforced with untreated coir fibers, whose deflection response peaked at approximately 0.2 mm for its 7 and 14-day specimens. The strain capacity of the composite samples to failure was enhanced as a result of this progressive increase in deflection. Consequently, the composite sample reinforced with 5% alkali-treated coir fiber (S6) exhibited the highest strain capacity to failure in comparison to its counterpart reinforced with 5 % untreated coir fiber as observed by Kameli *et al.* (2024).

4. CONCLUSION

This study investigated the reinforcing capability of treated and untreated fibers at varying percentages and the effects of treatment with 1, 2, and 3 M alkali concentrations for 2 hrs at ambient laboratory temperature. The TS and YM of recycled coir fibers was considerably enhanced by alkali solution treatment, resulting in a 63.14 % and 68.18 % increase, respectively, in comparison to the untreated fiber. As a result, it is deemed acceptable to treat recycled coir fibers with an alkali concentration of 2 M and a 2-hour immersion time

to enhance their surface characteristics and tensile properties. The FS of the 5 wt % treated coir fiber-reinforced composite board was 10.66 MPa, which is substantially greater than the minimum flexural strength (8.79 MPa) required for fiber cement flat sheet in accordance with the relevant standards. Additionally, the composite board demonstrated enhanced ductility. This composite sample can be recommended for use in affordable housing homes for interior construction purposes.

FUNDING

This research received no specific grant from any funding agency in the public, commercial, or not-for-profit sectors.

CONFLICT OF INTEREST

The authors declare that there is no conflict of interest.

COPYRIGHT

This article is an open-access article distributed under the terms and conditions of the Creative Commons Attribution (CC BY) license (http://creativecommons.org/licenses/by/4.0/).



REFERENCES

Abou, Y. H. and Kamel, S., Physico-mechanical properties of all-cellulose composites prepared by different approaches from micro-fibrillated bagasse pulp fibers, *Mater. Today. Commun.*, 35, 105672(2023). https://doi.org/10.1016/j.mtcomm.2023.105672

Akbulut, Z. F. and Guler, S., Enhancing the resilience of cement mortar, Investigating Nano-SiO_2 size and hybrid fiber effects on sulfuric acid resistance, *J. Build. Eng.*, 98, 111187(2024). https://doi.org/10.1016/j.jobe.2024.111187

Ali, B., Farooq, M. A., El-Ouni, M. H., Azab, M. and Elhag, A. B., The combined effect of coir and superplasticizer on the fresh, mechanical, and long-term durability properties of recycled aggregate concrete, *J. Build. Eng.*, 59, 105009(2022). https://doi.org/10.1016/j.jobe.2022.105009

Amsalu, F, T., Chande, J. Y. A., Kivevele, T. and Rahbar, N., A review on degradation improvement of sisal fiber by alkali and pozzolana for cement composite materials, *J. Nat. Fibers.*, 21(1), 2335327(2024). https://doi.org/10.1080/15440478.2024.2335327

Bheel, N., Kumar, S., Kirgiz, M. S., Ali, M., Almujibah, H. R., Ahmad, M. and Gonzalez, R. A., Effect of wheat straw ash as cementitious material on the mechanical characteristics and embodied carbon of concrete reinforced with coir fiber, *Heliyon.*, 10(2), e24313(2024). https://doi.org/10.1016/j.heliyon.2024.e24313

Bothiraj, T., Boopathi, K., Kalaiselvan, K., Benham, A. and Mayakannan, S., Experimental investigations on mechanical and wear behavior of waste marble dust and coconut fiber reinforced hybrid bio composites, *Mater. Today. Proc.*, 68, 2239–2242(2022). https://doi.org/10.1016/j.matpr.2022.08.441

Brasil, C. D. S. W., Barroso, S. H. D. A., De, P. S. L. G., Cabral, A. E. B. and Stefanutti, R., Potential application of by-products from the construction industry and waste from coconuts for concrete road paving blocks, physical and mechanical properties, *Int. J. Pavement. Eng.*, 25(1), 2424392(2024). https://doi.org/10.1080/10298436.2024.2424392

Dutta, T., Pandey, S. and Sengupta, H., In-depth exploration of utilizing water hyacinth fibers as a sustainable method for reinforcing concrete, *Sustainable Materials, Structures and IoT*, 1st Ed., 1-326(2024). https://doi.org/10.1201/9781003596776-7

Ehman, N. V., Nagy, D., Felissia, F. E., Vallejos, M. E., Quispe, I., Area, M. C. and Chinga, C. G., Biocomposites of Bio-Polyethylene Reinforced with a Hydrothermal-Alkaline Sugarcane Bagasse Pulp and Coupled with a Bio-Based Compatibilizer, *Mol.*, 25(9), 2158(2020). https://doi.org/10.3390/molecules25092158

Gavilanes, A., Noorvand, H., Hassan, M., Arce, G. and Rupnow, T., Incorporation of Cellulose Nanocrystals Synthesized from Rice Husk in Engineered Cementitious Composites, *Transp. Res. Rec. J.*, 2679(1), 1996-2014(2024). https://doi.org/10.1177/03611981241258749

Ghosh, S., Bansal, S., Choudhary, L. and Sahu, V., Effects of coconut fiber on mechanical properties of pervious concrete incorporating recycled concrete aggregates, *SSRN. Electron. J.*, 1-10(2024) https://doi.org/10.2139/ssrn.4865283

Hama, S. M., Hamadi, E. F. and Jahami, A., structural behavior of reinforced fibrous concrete beams incorporating nano silicon dioxide powder, *Eng. Rep.*, 7(1), e13078(2025). https://doi.org/10.1002/eng2.13078

Kameli, S., Shahi, A. H. and Mahboob, A., Investigating the mechanical properties of natural fiber-reinforced concrete with kenaf, jute and coconut fibers, *J. Civ. Eng. Res.*, 6(4), 32–39(2024). https://doi.org/10.61186/JCER.6.4.32

Lamichhane, N., Lamichhane, A. and Gyawali, T. R., Enhancing mechanical properties of mortar with short and thin banana fibers, A sustainable alternative to synthetic fibers, *Heliyon.*, 10(10), e30652(2024). https://doi.org/10.1016/j.heliyon.2024.e30652

Li, L., Jin, P., Zhang, K., Yan, C., Zhang, N., Li, Y. and Feng, Q., Influence of freeze–thaw cycles on fracture behaviors of Nano-SiO2 modified high-strength high- ductility alkali-activated material, *Theor. Appl. Fract. Mech.*, 135, 104774(2025). https://doi.org/10.1016/j.tafmec.2024.104774

Mahboob, A., Hassanshahi, O., Safi, M. and Majid, T. A., Experimental investigation of eco-friendly fiber-reinforced concrete using recycled and natural fibers, integrated with recycled aggregates, *Adv. Compos. Mater.*, 33(6), 1101–1130(2024). https://doi.org/10.1080/09243046.2024.2322799

Mahmood, A., Pechociakova, M., Noman, M. T., Wacławek, S., Gheibi, M., Behzadian, K., Wiener, J. and Militky, J., Aging behaviour assessment of cellulosic fibres in alkaline media, A green technology approach in construction materials, *J. Build. Eng.*, 92, 109685(2024). https://doi.org/10.1016/j.jobe.2024.109685

Mahmoud, A. E. W., Integrating fiber with new cement trends to create a greener future for sustainable concrete, *Glob. J. Eng. Technol. Adv.*, 21(2), 001–006(2024). https://doi.org/10.30574/gjeta.2024.21.2.0203

Maier, D., Manea, D. L., Tămas, G. D. R., Tiriac, A. and Costin, P., Wood–cement composites, A sustainable approach for mitigating environmental impact in construction, *J. Compos. Sci.*, 8(11), 474(2024). https://doi.org/10.3390/jcs8110474

Majumder, A., Stochino, F., Frattolillo, A., Valdes, M., Gatto, G. and Martinelli, E., Sustainable retrofitting solutions, evaluating the performance of jute fiber nets and composite mortar in natural fiber textile reinforced mortars, *Sustainability.*, 16(3), 1175(2024). https://doi.org/10.3390/su16031175

Mkilima, T., Sabitov, Y., Shakhmov, Z., Abilmazhenov, T., Tlegenov, A., Jumabayev, A., Turashev, A. and Kaliyeva, Z., Exploring the synergistic effect of recycled glass fibres and agricultural waste ash on concrete strength and environmental sustainability, *Clean. Eng. Technol.*, 20, 100752(2024). https://doi.org/10.1016/j.clet.2024.100752

Morsi, S. M. M., Abd, El. S. E. S., Ismail, A. and Kamel, S., Styrene/acrylate copolymer emulsions as strengthening agents for kraft bagasse pulp, A way for enhancing the mechanical properties of paper, *J. Appl. Polym. Sci.*, 141(17), e55290(2024). https://doi.org/10.1002/app.55290

Palanisamy, S., Murugesan, T. M., Palaniappan, M., Santulli, C. and Ayrilmis, N., Fostering sustainability, The environmental advantages of natural fiber composite materials, a mini review, *Environ. Res. Technol.*, 7(2), 256–269(2024). https://doi.org/10.35208/ert.1397380

Ramya, V. and Vijayaprabha, C., Investigation on mechanical behavior of engineered cementitious composites incorporating alkali-resistant glass fiber and quarry dust, *Struct. Concr.*, 25(5), 3866–3882(2024). https://doi.org/10.1002/suco.202301140

Siouta, L., Apostolopoulou, M. and Bakolas, A., Natural Fibers in Composite Materials for Sustainable Building, A state of the art review on treated hemp fibers and hurds in mortars, *Sustainability*, 16(23), 10368(2024). https://doi.org/10.3390/su162310368

Sridhar, R., Aosai, P., Imjai, T., Setkit, M., Shirkol, A. and Laory, I., Influence of Nanoparticles and PVA Fibers on Concrete and Mortar on Microstructural and Durability Properties, *Fibers*, 12(7), 54(2024). https://doi.org/10.3390/fib12070054

Sun, D., Fan, X., Xie, Y., Ren, X., Ding, F., Wu, R. and Ji, H., Experimental study and multi-objective optimization of the shear mechanical properties of recycled aggregate concrete with hybrid fibers and nano SiO2, *Constr. Build. Mater.*, 429, 136463(2024). https://doi.org/10.1016/j.conbuildmat.2024.136463

Yang, M., Chen, L., Lai, J., Osman, A. I., Farghali, M., Rooney, D. W. and Yap, P. S., Advancing environmental sustainability in construction through innovative low-carbon, high-performance cement-based composites, A review, *Mater. Today. Sustain.*, 26, 100712(2024). https://doi.org/10.1016/j.mtsust.2024.100712

Yeh, C. H., Wu, J. H. and Yang, T. C., Drying Shrinkage and Mechanical Strength of Cementitious Composites with Alkali-Treated Makino Bamboo Fibers, *J. Nat. Fibers.*, 21(1), 2321531(2024). https://doi.org/10.1080/15440478.2024.2321531

Zhang, G. -Z., Liu, C., Cheng, P. -F., Li, Z., Han, Y. and Wang, X. -Y., Enhancing the interfacial compatibility and self-healing performance of microbial mortars by nano-SiO2-modified basalt fibers, *Cem. Concr. Compos.*, 152, 105650(2024). https://doi.org/10.1016/j.cemconcomp.2024.105650

Zhang, J., Li, J., Zhang, L., Liu, Z. and Jiang, Z., Dynamic Performance of Foam Concrete With Recycled Coir Fiber, *Front. Mater.*, 7, 567655(2020). https://doi.org/10.3389/fmats.2020.567655

Zhu, M., Du, C., Yi, F., Tao, H., Cheng, C. and Jiang, J., Nano-modification of basalt fiber surface and its improvement on mechanical properties and salt resistance of cement-based materials, *Constr. Build. Mater.*, 472, 141000(2025). https://doi.org/10.1016/j.conbuildmat.2025.141000